Korean J. Chem. Eng., **31**(4), 639-643 (2014)
DOI: 10.1007/s11814-013-0286-2

pISSN: 0256-1115
eISSN: 1975-7220

Synthesis and characterization of Co and Mn doped NiO nanoparticles

Kaliyan Vallalperuman*,†, Mathivanan Parthibavarman*, Sekar Sathishkumar*, Manickam Durairaj*, and Kuppusamy Thavamani**

*Department of Physics, Mahendra Engineering College, Tiruchengode 637503, India
**Department of Physics, AVS Technical Campus, Salem 636106, India
(*Received 5 October 2013 • accepted 18 December 2013*)

Abstract−Diluted magnetic semiconductors (DMS) are intensively studied for their potential spintronics applications, especially those with Curie temperature above the room temperature. $Ni_{1-x}Mn_xO$ and $Ni_{1-x}Co_xO$ (x=1% & 2%), nanoparticles with size around 40-50 nm, were prepared by co-precipitation method. An NiO single phase structure was confirmed by powder X-ray diffraction measurements. Also, diffraction peaks show a systematic shift towards higher angle with an increase in Mn concentration, which is associated with the lattice variation. The samples were pelleted and examined for its magnetic property using a vibrating sample magnetometer (VSM); it indicates paramagnetic-like behavior at room temperature. The increase in a.c conductivity with increasing temperature is attributed to the increase in drift mobility of the charge carriers.

Keywords: Diluted Magnetic Semiconductors, Nanocrystalline, Crystal Structure, Vibrating Sample Magnetometer

INTRODUCTION

Diluted magnetic semiconductors (DMS) are extensively investigated nowadays due to their potential for use in spintronic devices [1-4]. In these devices, the spin of carriers, along with the charge, is an active element for transmitting and storing information, which makes it possible to increase the speed and memory of computer chips by orders of magnitude. "Spintronics" (spin based electronics), which employs the interplay between the electronic and the magnetic property of semiconductors, has kept rapidly developing [4,5]. Spintronic materials should have high Curie temperatures, high spin polarization of charge carriers, and compatibility with semiconductors.

There has been considerable recent interest in the design of high Curie temperature DMS with a particular focus on the oxide-based DMSs, e.g., ZnO, TiO_2, SnO_2, In_2O_3, etc., with various transition metals (TM) [6,7]. It is generally believed that magnetic ordering in oxide based DMSs appears sensitive to chemical ordering of the TM dopants, carrier concentration, and defects such as vacancies and interstitials [8-10]. Ferromagnetic (FM) properties, stabilized or enhanced by the co doping ions, have been predicted theoretically and confirmed by some experiments. Sato and Yoshida [11] used first principles calculations to reveal that Mn-doped ZnO can change its magnetic state from the spin-glass state to the FM state with increasing hole concentration. Dietl et al. [12] used Zener's model to predict ferromagnetism in p-type Mn-doped ZnO and found that ferromagnetism was driven by the exchange interaction between hole charge carriers and localized spins.

Intensive studies have been conducted on the preparation of transition metal doped NiO nanocrystals and thin films using chemical vapor phase depositions to understand the origin of room-temperature ferromagnetism in DMSs. In some of the materials, room-temperature ferromagnetism was explained in terms of the carrier-induced ferromagnetism, double exchange mechanism. However, the magnetic contributions from the secondary phases of component transition metal oxide nanocrystals were always excluded as a likely source under the consideration that the component oxides (NiO, CoO) were generally antiferromagnetic and most of the nanoscale counterparts would only exhibit ferromagneticlike behavior at very low temperatures such as at 4.2 K, due to the low Curie temperature (e.g., TC<5 K for 3.1 nm NiO) [13].

So far, room temperature (RT) ferromagnetism has been observed in a variety of transition metal-doped oxides, such as TiO_2, ZnO, Cu_2O, SnO_2, and In_2O_3. However, most of the RT ferromagnetic diluted magnetic semiconducting (DMS) materials have noncubic crystal symmetry. It is anticipated that if one could introduce room temperature ferromagnetism in cubic systems, it would facilitate the integration of spintronic devices with advanced silicon based microelectronic devices.

The transition metal oxide nanocrystals (NiO) are noticeably comparable to those for thin films [14]. Experimental verification of room-temperature ferromagnetism of the transition metal oxide nanocrystals as a function of their crystallite size can be expected to have many implications in understanding the origins of room temperature ferromagnetism in DMS nanostructures. Therefore, we chose NiO as the target material because it has lattice, magnetic and structural similarities to that of transition metal oxides (CoO, FeO, and MnO) that could be possible component oxides in DMSs [15-18]. Mn and Co doped NiO nanocrystals with two different compositions were prepared systematically by the chemical co-precipitation technique, and basic investigation such as crystal structure, electrical and magnetic properties were carried out. The origin of ferromagnetism in Mn and Co doped NiO has been under persistent question over the years. This result demonstrates a pronounced paramagnetic contribution at room temperature at particle sizes larger than 50 nm.

†To whom correspondence should be addressed.
E-mail: vallalphysics1@gmail.com

2. Sample Preparation

Samples with stoichiometry $Ni_{0.99}Mn_{0.01}O$, $Ni_{0.98}Mn_{0.02}O$, $Ni_{0.99}Co_{0.01}O$ and $Ni_{0.99}Co_{0.02}O$ were prepared by the chemical co-precipitation technique. High purity $NiCl_2.6H_2O$ (Aldrich 99.999%), $CoCl_2 \cdot 6H_2O$ (Aldrich 99.999%), and $MnCl_2 \cdot H_2O$ (Aldrich 99.999%), were weighed and dissolved in de-ionized water. The solutions prepared from the starting materials were taken in a round-bottomed flask fitted with a reflex-cooling tube. Then, an aqueous 500 ml NaOH solution of 5 mol/*l* was gradually added to the stoichiometric solution for 30 minutes, in order to achieve a final pH value of 8 at room temperature. The precipitates containing mixture were allowed to settle for a reasonable time and then washed several times with pure water to remove the water-soluble by products (peptization). Now, the precipitates were filtered out using filter paper of fine pore size and the spongy content in the filter cone was allowed to dry as such. When the moisture content was reduced, the sample could also be dried (calcination) in a ceramic pan at about 50 °C to help the remnant moisture and traces of by-products to evolve out of the sample completely. Now the sample was ready for further treatment and study. Then dried powders were annealed at various temperatures (600 °C, 700 °C and 800 °C) for 4 hrs in air and optimized temperature is 800 °C. To verify the composition of resultant powder, inductively coupled plasma optical emission spectroscopy (ICP-OES) technique was carried out. It confirmed the absence of impurities. X-ray diffraction was used to determine different phases and lattice parameters of the nanostructures. The X-ray scan was conducted under Cu Kα (λ=1.54056 Å) radiation at a scan rate of 0.05° 2θ steps per second from 20° to 80°. The electrical properties of the samples were studied using impedance analyzer (Solatron 1260 Impedance/gain-phase analyzer. Vibrating sample magnetometer (Lakeshore VSM 7410) was used to investigate the magnetic properties of the co-precipitated nanocrystalline samples. The crystallite size and morphology were analyzed using transmission electron microscopy (TEM).

RESULTS AND DISCUSSION

1. XRD Results

Powder X ray diffraction technique plays a vital role for any sample, prepared by any method to identify the phase formation. Figs. 1 and 2 show the XRD measurements on samples $Ni_{0.99}Co_{0.01}O$, $Ni_{0.98}Co_{0.02}O$, $Ni_{0.99}Mn_{0.01}O$ and $Ni_{0.98}Mn_{0.02}O$ (heat treated at 800 °C 4 hrs in air) using Cu K_α radiation confirm the cubic structure of NiO. The lattice parameter value 'a' of the samples was calculated to be 4.176 (1) Å for $Ni_{0.99}Co_{0.01}O$, 4.178 (3) Å for $Ni_{0.98}Co_{0.02}O$ (Fig. 1). No significant variation was found in the lattice parameters of doped samples when compared to that of un-doped NiO (JCPDS # 78-0643]. This is because the ionic radii of Ni^{2+} ion (0.69 Å) are comparable to that of Co^{2+} ion (0.72 Å).

It is evident from Fig. 2 that the lattice parameter values 'a' of the samples were 4.172 (2) Å for $Ni_{0.99}Mn_{0.01}O$, and 4.176 (1) Å for $Ni_{0.98}Mn_{0.02}O$, which agrees well with that reported for NiO [JCPDS # 78-0643]. Also, diffraction peaks show a systematic shift towards higher angle with an increase in Mn concentration, which is associated with the lattice variation. This slight variation in lattice parameter values proves that Mn ions are indeed incorporated into the NiO lattice. As the annealing temperature is increased, crystallization is induced, stress and strain are relieved and hence grain growth occurs.

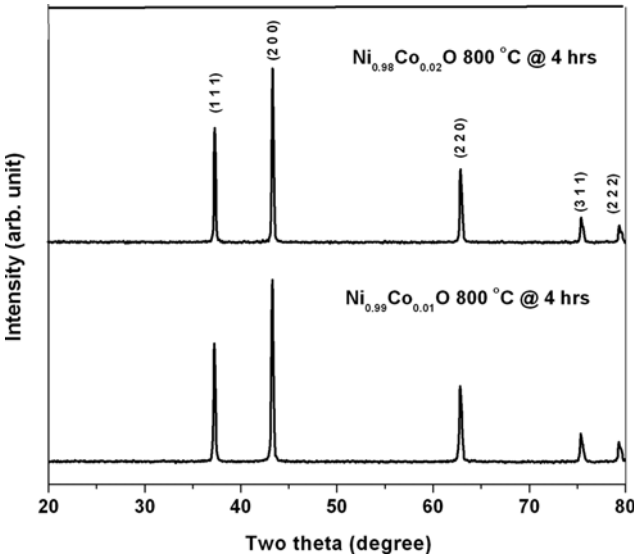

Fig. 1. XRD pattern of $Ni_{0.99}Co_{0.01}O$ and $Ni_{0.98}Co_{0.02}O$ annealed at 800 °C for 4 hrs in air.

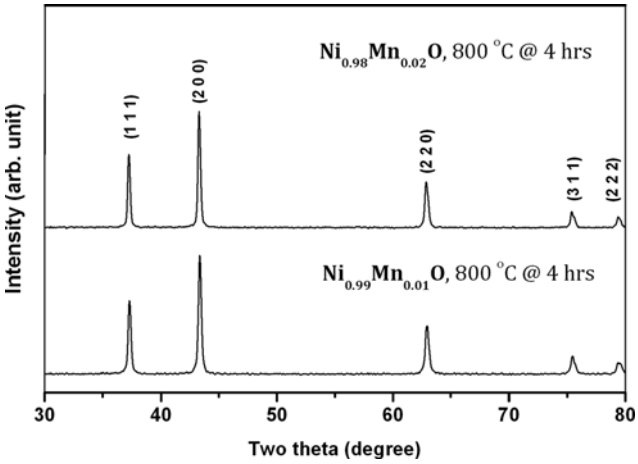

Fig. 2. XRD pattern of $Ni_{0.99}Mn_{0.01}O$ and $Ni_{0.98}Mn_{0.02}O$ annealed at 800 °C for 4 hrs in air.

This is evident from the gradual increase in the intensity as well as sharpness of the line and decrease in FWHM of the peaks in XRD pattern.

To determine the average particle size t, we have taken into account the Scherrer formula $t=(0.9\lambda/\beta\cos\theta)$ where 'θ' is the Bragg angle and 'β' is the full width at half maxima, λ=1.5418 Å in the Cu K_α radiation. The average crystallite size of $Ni_{0.99}Mn_{0.01}O$ and $Ni_{0.98}Mn_{0.02}O$, is obtained using Scherrer's relation [19], which is 44 nm and 48 nm, respectively.

2. VSM Results

The magnetic behavior of the samples was studied by using a vibrating sample magnetometer (VSM) at room temperature with a maximum applied field of 7 kOe. Initially, a fresh empty sample holder was swept to record the diamagnetic contribution, which was then subtracted from the signal obtained for sample kept in the sample holder and the appropriate correction was given while plotting the data. Figs. 3 and 4 present the M-H curve plot of $Ni_{0.99}Co_{0.01}O$, $Ni_{0.98}Co_{0.02}O$, $Ni_{0.99}Mn_{0.01}O$ and $Ni_{0.98}Mn_{0.02}O$ (heat treated at 800 °C 4 hrs in air).

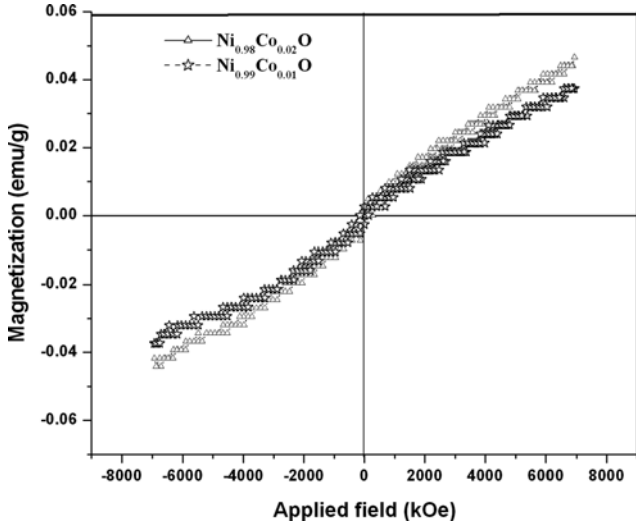

Fig. 3. M-H curve of $Ni_{0.99}Co_{0.01}O$ and $Ni_{0.98}Co_{0.02}O$ (800 °C/4 hrs) at room temperature.

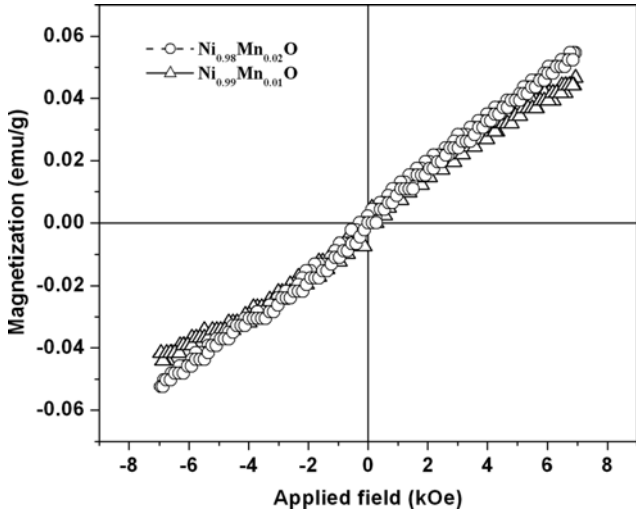

Fig. 4. M-H curve of $Ni_{0.99}Mn_{0.01}O$ and $Ni_{0.98}Mn_{0.02}O$ (800 °C/4 hrs) at room temperature.

A clear paramagnetic behavior is observed for both the samples, similar to the observations in many of the reports where paramagnetic behavior was reported without any evidence of a ferromagnetic ordering, by means of Mn, and Co doping in various semiconductor hosts [20-24].

Makhlouf et al. observed the ferromagnetic behavior in NiO nanoparticles with diameter of less than 8 nm because of the finite size effect. They also stated that the ferromagnetic signature disappeared for NiO particles of larger than 30 nm size [3]. No such finite size effect could be observed for our samples having average crystallite size of 40 nm. This also agrees with the report of Makhlouf et al., which shows that the ferromagnetic signature is absent in NiO particles of size larger than 30 nm. At low temperatures, a better magnetic signal indicating ferromagnetic ordering is expected to occur in most of the materials. Raja et al. have observed ferromagnetic behavior at 77 K and paramagnetic behavior at room temperature for Mn doped CuO samples [24,25]. CuO is an antiferromagnetic semiconductor with a Neel temperature of 230 K, and hence the magnetic interaction at room temperature and at low temperature (77 K) will be quite distinguishable. But as far as NiO is concerned, this is not possible. The antiferromagnetic ordering of NiO remains the same even when the temperature is lowered because of its high Neel temperature [TN=523 K].

Therefore, if the doping of Mn ions could not lead to ferromagnetic ordering at room temperature by altering the antiferromagnetic interaction in NiO, it is also expected not to give rise to any ferromagnetic behavior at low temperature. Grain size of the sample plays the major role in attaining FM behavior. From VSM results, the finite size effect that could lead to a ferromagnetic behavior of NiO can be completely ruled out in these samples. According to Makhlouf et al., no such effect was observed for NiO particles of larger than 40 nm [23]. This agrees with our magnetic results as the average crystallite size of the samples is ~50 nm.

At low temperatures, a better magnetic signal indicating ferromagnetic ordering is expected to occur in most of the materials. Raja et al. observed ferromagnetic behavior at 77 K and paramagnetic behavior at room temperature for Mn doped CuO samples [24]. CuO is an antiferromagnetic semiconductor with a Neel temperature of 230 K, and hence the magnetic interaction at room temperature and at low temperature (77 K) was quite distinguishable. But as far as NiO is concerned, this may not be possible. The antiferromagnetic ordering of NiO remains the same even when the temperature is lowered because of its high Neel temperature [TN=523 K]. Therefore, if the doping of Co, Mn ions could not lead to the ferromagnetic ordering at room temperature by altering the antiferromagnetic interaction in NiO, it is also expected not to give rise to any ferromagnetic behavior at low temperature. Further characterization will be dealt with only for $Ni_{0.98}Co_{0.02}O$ and $Ni_{0.98}Mn_{0.02}O$ samples annealed at 800 °C for 4 hrs, which have phase pure nature as evident from XRD results.

3. The a.c. Conductivity Studies

The a.c. conductivity of $Ni_{0.98}Co_{0.02}O$ sample was measured in a wide frequency range at different temperatures. The frequency dependence of the conductivity at various temperatures is shown in Figs.

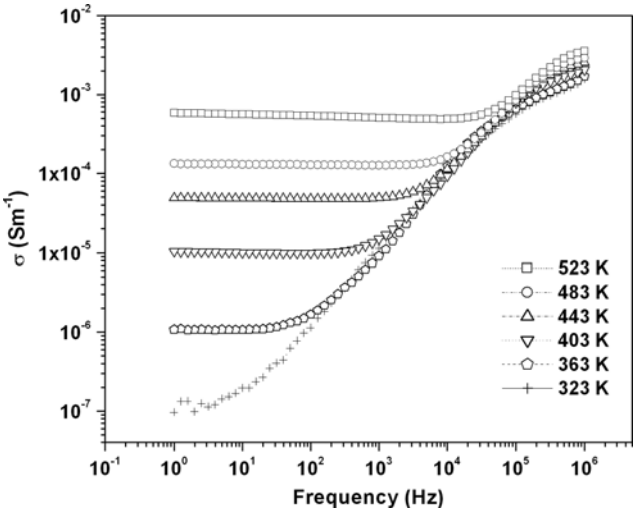

Fig. 5. a.c. Conductivity of $Ni_{0.98}Co_{0.02}O$ as a function of frequency at various temperatures.

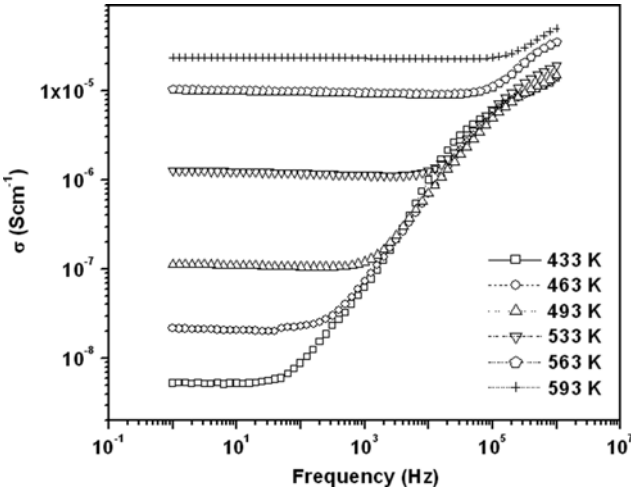

Fig. 6. a.c. Conductivity of $Ni_{0.98}Mn_{0.02}O$ as a function of frequency at various temperatures.

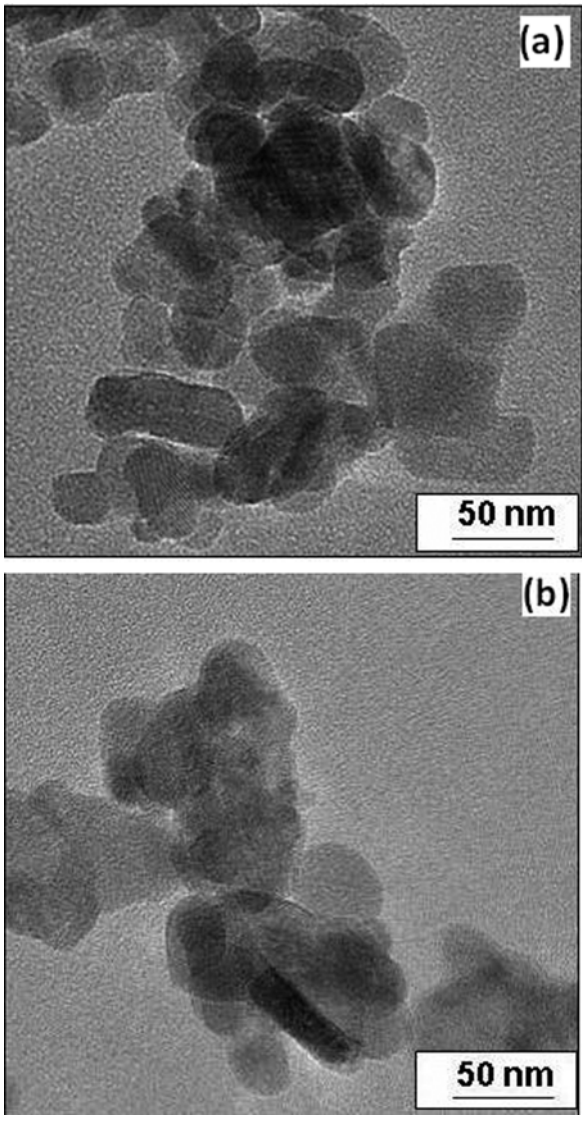

Fig. 7. (a) And (b) the low magnification TEM micro graph of $Ni_{0.98}Co_{0.02}O$ and $Ni_{0.98}Mn_{0.02}O$ nanoparticles annealed at 800 °C for 4 hrs in air.

5 and 6. The conductivity is found to be frequency independent in the low frequency region ($\omega<\omega p$). This frequency independent conductivity is equal to the d.c. conductivity. When the frequency exceeds the hopping frequency wp, conductivity (σ_{ac}) increases with frequency following the power law dispersion $\sigma_{ac} \propto w^n$ (where n<1) [26]. It is observed that the plateau region gets shifted towards higher frequencies as the temperature is increased. The increase in electrical conductivity with temperature is attributed to the drift mobility of the thermally activated charge carriers according to hopping mechanism.

4. TEM Analysis

Fig. 7(a) and (b) show the low magnification TEM micro graph of $Ni_{0.98}Co_{0.02}O$ and $Ni_{0.98}Mn_{0.02}O$ nanocrystals particles synthesized at calcination temperature of 800 °C. The particles are nearly spherical with varying particles size from 40 to 50 nm, which is consistent with average crystalline sizes of 44 and 48 nm, calculated using the Scherrer formula according to the XRD.

CONCLUSIONS

Co and Mn doped NiO were prepared for different composition by chemical co-precipitation method. Single phase was obtained for $Ni_{1-x}Co_xO$ and $Ni_{1-x}Mn_xO$ (x=1% & 2%), annealed at 800 °C/4 h in air. Paramagnetic behavior was observed for $Ni_{0.99}Mn_{0.01}O$ and $Ni_{0.98}Mn_{0.02}O$ using vibrating sample magnetometer. Ferromagnetic signature disappeared for NiO particles larger than 40 nm. Impedance spectroscopy measurements were also carried out to study the electrical properties of the samples. Power law dispersion is obeyed with frequency independent plateau region extending towards higher frequency values with an increase in temperature.

ACKNOWLEDGEMENTS

One of the authors (K. Vallalperuman) would like to thank Prof. Dr. C. Venkateswaran, Dept. of Nuclear Physics, Madras University for introducing him to the subject and constant encouragement throughout the research journey.

REFERENCES

1. R. Aruna, P. Kalaivanan and K. Gnanasekar, *Super Lattices and Microstructures*, **52**, 1020 (2012).
2. M. K. Li, S. J. Lee, S. U. Yuldashev, G. Ihm and T. W. Kang, *J. Magn. Magn. Mater.*, **323**, 2639 (2011).
3. S. A. Wolf, D. D. Awschalom, R. A. Buhrman, J. M. Daughton, S. Molnar, M. L. Roukes, A. Y. Chtchelkanova and D. M. Treger, *Science*, **294**, 1488 (2001).
4. Y. Kobayashi, J. Ishida, I. Hwang, T. Mizokawa, A. Fujimori, K. Mamiya, J. Okamoto, Y. Takeda, T. Okane, Y. Saitoh, Y. Muramatsu, A. Tanaka, H. Saeki, H. Tabata and T. Kawai, *Phys. Rev. B*, **72**, 201201 (2005).
5. A. Kurokawa, N. Sakai, L. Zhu, H. Takeuchi, S. Yano, T. Yanoh, K. Onuma, T. Kondo, K. Miike, T. Miyasaka and Y. Ichiyanagi, *J. Korean Phys. Society*, **63**, 716 (2013).
6. S. B. Ogale, R. J. Choudhary, J. P. Buban, S. E. Lofland, S. R. Shinde, S. N. Kale, V. N. Kulkarni, J. Higgins, C. Lanci, J. R. Simpson, N. D. Browning, S. Das Sarma, H. D. Drew Greene and T. Venkatesan,

Phys. Rev. Lett., **91**, 077205 (2003).
7. J. Philip, A. Punnoose, B. I. Kim, K. M. Reddy, S. Layne, J. O. Holmes, B. Satpati, P. R. Leclair, T. S. Santos and J. S. Moodera, *Nat. Mater*., **5**, 298 (2006).
8. W. Prellier, A. Fouchet and B. Mercey, *J. Phys.: Condens. Matter*, **15**, R1583 (2003).
9. M. Venkatesan, C. B. Fitzgerald and J. M. D. Coey, *Nature London*, **430**, 630 (2004).
10. A. Dana Schwartz and R. Daniel, *Adv. Mater.*, **16**, 2115 (2004).
11. K. Sato and H. K. Yoshida, *Semi Cond. Sci. Technol*., **17**, 367 (2000).
12. T. Dietl, H. Ohno, F. Matsukura, J. Cibert and D. Ferrand, *Science*, **287**, 1019 (2000).
13. R. A. Winston and J. F. Cordaro, *J. Appl. Phys*., **68**, 6495 (1990).
14. S. B. Zhang, S. H. Wei and A. Zunger, *Phys. Rev. B*, **63**, 075205 (2001).
15. S. Mohanty and S. Ravi, *Solid State Communications*, **150**, 1570 (2010).
16. Y. Kalyana Lakshmi, K. Srinivas, B. Sreedhar, M. Manivel Raja, M. Vithal and P. Venugopal Reddy, *Mater. Chem. Phys.*, **113**, 749 (2009).
17. B. D. Cullity, *Elements of X-ray diffraction*, Addison-Wesley, Reading, MA, 98 (1956).
18. S. Kolesnik, B. Dabrowski and J. Mais, *J. Appl. Phys*., **95**, 2582 (2005).
19. A. Tiwari, C. Jin, A. Kwit, D. Kumar, J. F. Muth and J. Narayan, *Solid State Commun*., **121**, 371 (2002).
20. X. M. Cheng and C. L. Chien, *J. Appl. Phys*., **93**, 7876 (2003).
21. C. N. R. Rao and F. L. Deepak, *J. Mater. Chem*., **15**, 573 (2005).
22. D. Paul Joseph, G. Senthilkumar and C. Venkateswaran, *Mater. Lett.*, **59**, 2720 (2005).
23. S. A. Makhlouf, F. T. Parker, F. E. Spada and A. E. Berkowitz, *J. Appl. Phys*., **81**, 5561 (1997).
24. S. Philip Raja, D. Paul Joseph and C. Venkateswaran, *Mater. Chem. Phys.*, **113**, 67 (2009).
25. S. S. Nkosia, B. Yalisia, D. E. Motaung, J. Keartland, E. Sideras-Haddad, A. Forbes and B. W. Mwakikunga, *Appl. Surface Sci.*, **265**, 860 (2013).
26. D. P. Almond and A. R. West, *Solid State Ionics*, **9-10**, 277 (1983).